Chapter 3.

OFDM for Digital Broadcasting Applications

Contents

The high spectral efficiency and the robustness against multipath effects, combined with simplified channel estimation, have made OFDM a very popular modulation scheme. It can be encountered in digital broadcasting, such as DVB-T, DAB, or DRM, as well as in wireless networking applications, such as IEEE 802.11a/g. A special category is the downlink channel in multiple-access wireless networks, like IEEE 802.16a, which has similar characteristics with digital broadcasting.

The chapter starts with a discussion regarding the specifics of OFDM for digital broadcasting in contrast with OFDM for wireless networks. It then goes on to propose a generic architecture

for OFDM broadcasting receivers which includes synchronization and channel estimation in the inner receiver, as well as symbol demapping and FEC correction in the outer receiver. The chapter concludes with a case study of three broadcasting standards that employ OFDM modulation, with emphasis on those properties that are essential for synchronization and channel estimation.

3.1. Specifics of Digital Broadcasting

This section discusses the specific issues when using OFDM for digital broadcasting, among which the most important are the continuous stream structure, the reference pilots, and the synchronization strategy in two phases.

Most wireless networks, such as the IEEE 802.11a LAN, employ packet-based communication. The data is divided into smaller chunks called packets, which are then transmitted sequentially. The packets are formed in the MAC (medium access controller) layer and processed for transmission in the PHY (physical) layer according to the specific environment, such as cable, radio, or infrared. In a wireless network, the PHY layer is responsible for channel coding and modulation.

In OFDM wireless networks, a packet is transmitted as a burst of contiguous OFDM symbols, preceded by preamble which consists of a few training symbols used for various synchronization purposes as well as for channel estimation. Dedicated training symbols are required because the synchronization has to be established very fast. In IEEE 802.11a for example, the preamble has two identical short training symbols (STS), used for packet detection and timing synchronization, followed by two identical long training symbols (LTS), used for frequency synchronization and channel estimation.

In a broadcasting scenario, however, data is not transmitted in bursts, but as a continuous stream with constant data rate. There are no special training symbols like in the case of a burst transmission. Therefore, the algorithms for synchronization and channel estimation differ significantly. The specific properties of OFDM for broadcasting are described in the following sections.

3.1.1. Stream Structure

As with any OFDM system, the data is transmitted as a series of of contiguous OFDM symbols. Unlike wireless packet-networks, where synchronization needs to be achieved fast, there are no dedicated symbols for synchronization. Instead, since the synchronization speed is not very critical, reference data is spread across multiple symbols.

Instead of burst packets, the continuous broadcasting stream is divided into frames, each frame

consisting of a fixed number of OFDM symbols. In the following, the number of symbols per frame is denoted by N_{spf}. The data stream is limited in frequency, due to the finite number of subcarriers, from k_{min} to k_{max}, but unlimited in time.

An (s, k) pair, corresponding to OFDM symbol s and subcarrier k, is referred to as an OFDM cell. The number of cells in a broadcasting frame is thus $N_{cpf} = N_{spf} \cdot (k_{max} - k_{min})$, considering that the DC subcarrier is not transmitted. Some of the cells, referred to as pilots or references, have known values and are used for various synchronization purposes and channel estimation. Since they do not carry information, the efficiency of the system is decreased.

The complex values of the pilots, denoted by $P_{s,k}$, are taken from a very limited alphabet, usually $1+j0$ or $-1+j0$. The pilots are usually scrambled by a pseudo-random binary sequence, in order to destroy their periodicity which would otherwise result in discrete components in the signal spectrum. Moreover, the pilots may have a boosted power level compared to other cells, which ensures a higher SNR and a better estimation. For example, the power boost is 16/9 for DVB-T and $\sqrt{2}$ for DRM.

For a given mode of operation, the pilot cells have well determined positions in the data stream. According to their purpose, there are typically three types of pilot references: timing references, frequency references, and gain references. For illustrative purposes, **Figure 3.1** shows an example of how the reference cells are located in a frame.

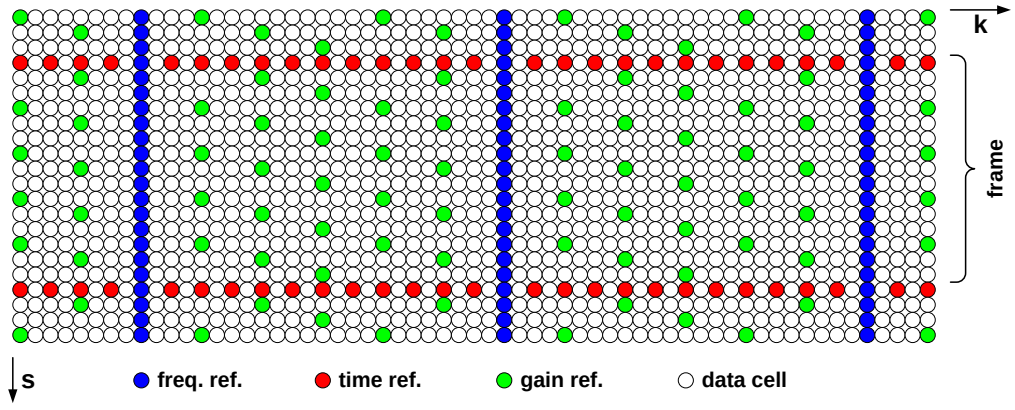

Figure 3.1.: Reference cells in a broadcasting OFDM frame

The *timing references* are present in the first OFDM symbol of each frame and are used for frame synchronization in the receiver. They should guarantee a reliable detection of the frame boundaries even at very low SNR's. The *frequency references*, also referred to as continuous pilots, are present in all symbols on the same subcarriers. They are used mainly for frequency and timing synchronization. The *gain references*, also called scattered pilots, are typically used for channel estimation and automatic gain control. Due to their importance in channel estimation, they are treated in more detail in **Section 3.1.2**.

3.1.2. Scattered Pilots

It has been shown in **Subsection 2.1.5** that the channel transfer function varies both in frequency due to the channel delay spread and in time because of the Doppler variation of the multipath components. The scattered pilots essentially perform a bi-dimensional sampling of the time-variant CTF. When sampling bi-dimensional data, not only the sampling periods for the two directions must be specified, but also the shape of the sampling grid.

For the characterization of the pilot sampling grid, we adopt the formalism presented in [62], which establishes a matrix notation for the general case of a N-D sampling. For the 2-D case, the sampling grid is specified by means of a 2×2 square matrix $\mathbf{V}$, which is referred to as the sampling matrix.

Each location (x_s, y_s) on the sampling grid can be then expressed in the condensed form as:

$$\mathbf{s} = \mathbf{V}\mathbf{n} \tag{3.1}$$

or in its expanded form as:

$$\begin{bmatrix} x_s \\ y_s \end{bmatrix} = \begin{bmatrix} V_{xx} & V_{xy} \\ V_{yx} & V_{yy} \end{bmatrix} \begin{bmatrix} n_x \\ n_y \end{bmatrix} \tag{3.2}$$

where each pair of integers (n_x, n_y) is mapped to a distinct point (x_s, y_s) on the sampling lattice. For a given lattice, the sampling matrix $\mathbf{V}$ is not unique. However, the quantity $|\det \mathbf{V}|$ is unique for a given lattice and it physically corresponds to the reciprocal of the sampling density.

For OFDM, the x axis is the symbol index s, whereas the y axis corresponds to the carrier index k. The most common pilot sampling grid is the rectangular one, for which $\mathbf{V}$ is diagonal.

$$\mathbf{V} = \begin{bmatrix} D_s & 0 \\ 0 & D_k \end{bmatrix} \tag{3.3}$$

The elements on the main diagonal represent the distances between pilots on the s and k axes. Although simple and interesting from a theoretical point of view, the rectangular grid is not very popular in practice since the number of data cells is not the same for all symbols. Most OFDM standards define a slanted grid instead, for which $\mathbf{V}$ has the expression

$$\mathbf{V} = \begin{bmatrix} D_s & 1 \\ 0 & D_k \end{bmatrix} \tag{3.4}$$

The pilot density is the same in both cases, its value being $1/D_x D_y$. **Figure 3.2** shows the resulting pilot grids for the two cases, with $D_s = 4$ and $D_k = 3$. In this example, the resulting pilot density is 1/12, as it can also be seen from the figures.

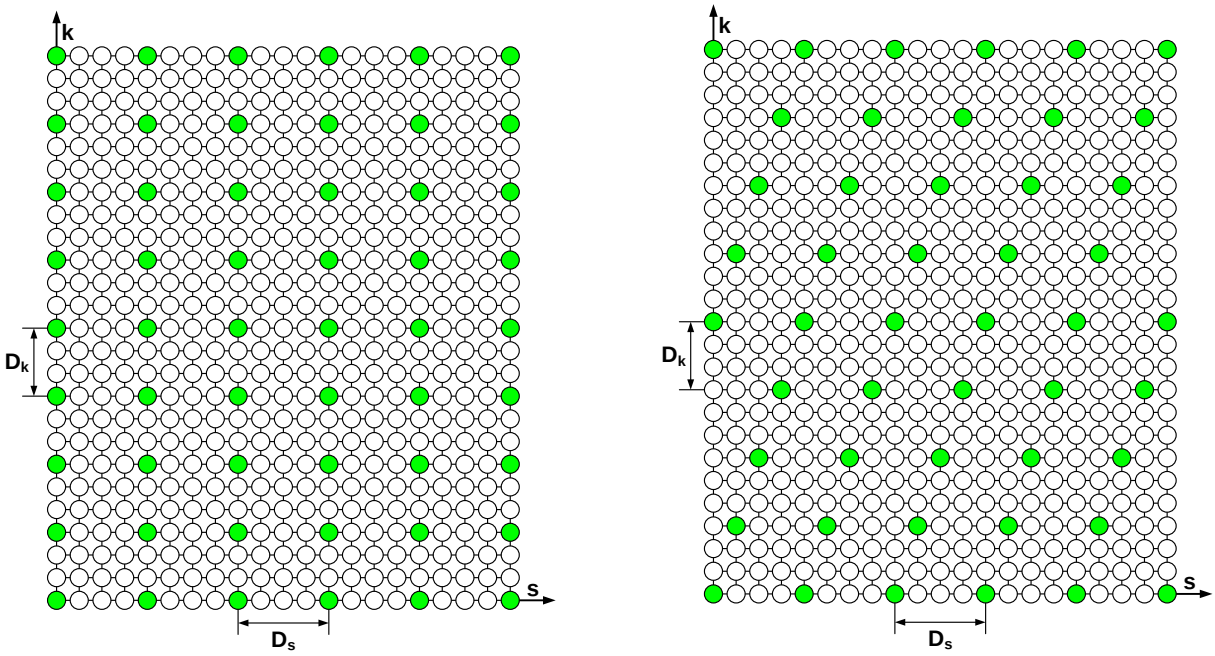

(a) Rectangular pattern

(b) Tilted pattern

Figure 3.2.: Scattered pilots patterns

When generating or extracting the pilots, it is necessary to tell if a certain OFDM cell in the frame, identified by its (s, k) coordinates, is a pilot. For the rectangular grid, this condition is straightforward and can be written as:

$$s \oplus D_s = 0 \tag{3.5}$$

$$k \oplus D_k = 0 \tag{3.6}$$

The $\oplus$ operator indicates the modulus after division. In the case of a slanted pilot grid, the expression is more complicated. In order to obtain it, we write the grid generation matrix equation as a system of two equations:

$$\begin{cases} s_p = D_s n_s + n_k \\ k_p = D_k n_k \end{cases} \tag{3.7}$$

By eliminating n_k between the two equations we obtain:

$$s_p D_k = D_s D_k n_s + k_p \tag{3.8}$$

Constraining n_s to be an integer we obtain the following condition for a given cell (s, k) to be a pilot cell (s_p, k_p):

$$(k - D_k s) \oplus D_s D_k = 0 \tag{3.9}$$

From this equation, it results that s may take any integer value, whereas k is always a multiple of D_k. For a given s, the distance between pilots in frequency is $D_s D_k$, the exact positions of

the pilots being given by the following equation:

$$k_p = D_k(s \oplus D_s) + D_s D_k n \tag{3.10}$$

where n is an integer.

The pilot spacing in time D_s and frequency D_k must ensure that CTF is sufficiently sampled, so that the sampling theorem is fulfilled for both directions. The variations of the CTF in time direction result from the Doppler variations of the multipath components, with rate f_D. The Doppler variation is sampled with the symbol period T_U multiplied by the pilot spacing D_s, so that the Nyquist condition can be written as:

$$f_D < \frac{1}{2D_s T_S} \tag{3.11}$$

Using the normalized value of the Doppler frequency f_{Dn}, the above equation can be written as:

$$f_{Dn} < \frac{1}{D_s(N_U + N_G)} \tag{3.12}$$

The variations of the CTF in frequency direction result from the time-dispersive nature of the multipath channel. More concretely, the channel transfer function (CTF) is the Fourier transform of the channel impulse response (CIR). As in the case of time-direction variations, the CTF must sufficiently sampled, so that the sampling theorem is fulfilled:

$$\tau_{max} < \frac{T_U}{D_k} \tag{3.13}$$

where τ_{max} is the maximum delay spread of the multipath channel.

If the length of the CIR in samples is denoted by L, corresponding to τ_{max}, the above equation can be written as:

$$L < \frac{N_U}{D_k} \tag{3.14}$$

Knowing that the length of the guard interval N_G is chosen according to the CIR length L, so that in the worst case $N_G = L$, the following condition must be fulfilled: $D_k > N_U/N_G$.

Having established the conditions that must be fulfilled by D_s and D_k, we introduce the over-sampling factors in time and frequency direction as:

$$r_s = \frac{1}{D_s f_{Dn}(N_U + N_G)} > 1 \tag{3.15}$$

and

$$r_k = \frac{N_U}{D_k L} > 1 \tag{3.16}$$

The above discussion is applicable in the case of a rectangular scattered pilot grid. For the slanted grid, the only additional constraint is that the channel has to be estimated first in time direction, for all subcarriers that contain pilots, then in frequency direction, for all symbols. This is necessary since the pilot spacing in frequency direction is actually $D_s D_k$ for every symbol.

3.1.3. Synchronization Strategy

The synchronization in OFDM involves to distinct aspects: timing and frequency synchronization. The former consists in finding and extracting the useful part of the symbol from the incoming signal, so that the inter-symbol interference (ISI) is minimized or completely eliminated. The latter involves the estimation and the compensation of the carrier and sampling clock frequency offsets, so that the inter-carrier interference (ICI) is minimized.

As already mentioned, the synchronization algorithms for digital broadcasting differ considerably from those encountered in burst packet-based wireless networks. In both applications, however, the synchronization is performed in two distinct steps. The first step, called acquisition, assumes that nothing is known about the parameter to be estimated. Its task is to roughly estimate and correct the parameter in order to bring it into a narrower range. The second step, called tracking, has a higher accuracy than the acquisition, but the parameter to be estimated must be in a more restricted range. The task of the acquisition is to bring the unknown parameter to a range from where the tracking algorithm can take over.

The acquisition process needs to be performed fast and reliably. Here, the acquisition time is the main optimization criterion and depends on the initial tolerance of the parameter to be estimated. For the tracking process, however, the emphasis is more on achieving high estimation accuracy.

In data-aided (DA) mode, the acquisition time also depends strongly on the density of the reference data. In packet-based networks, where data is transmitted in bursts, the acquisition needs to be performed very fast. The solution is to use special training symbols in the preamble of each packet, so that when the first data symbol arrives the synchronization is already achieved. In broadcasting applications, the acquisition is performed only once, whenever the receiver tunes on a new channel. The acquisition time is not very critical, so that the scattered references with lower density can be used for this purpose.

In the case of timing synchronization, the acquisition process exploits the periodicity of the cyclic prefix only. At this stage, it is not possible to rely on reference pilots since the frequency synchronization has not been yes achieved. Although strongly affected by noise and channel multipath effects, this class of algorithms achieves sufficient precision to enable frequency synchronization. When frequency synchronization has been achieved, the incremental rotation of the pilots within one OFDM symbol can be used to adjust the timing with a higher accuracy.

In the case of frequency synchronization, the acquisition algorithm has to deal with frequency offsets that can be as large as a few carrier spacings. A typical algorithm is the one presented in [11], which relies on the fact that the sum of the (s, k) symbols for those k with frequency references is maximum when the carrier offset is zero. The algorithm involves a search for maximum by varying the value of the frequency compensation. The tracking algorithm also relies on the continuous frequency references (see **Figure 3.1**), by evaluating their incremental rotation between two consecutive OFDM symbols. Using (**2.44**) (see also **Figure 2.20**), both the carrier and the sampling frequency offset can be estimated. The estimates are then used in control loops (PI, PLL, DLL) that minimize these offsets.

3.2. Broadcasting OFDM Transmitter

3.2.1. QAM Mapping

The complex data cells in **Figure 3.1** belong to a finite alphabet and are usually generated by quadrature amplitude modulation (QAM). The size of the constellation, and therefore the number of bits mapped to a symbol, depends on the SNR of the channel. Typical QAM constellations include 4-QAM, 16-QAM, and 64-QAM, which modulate 2, 4, and 6 bits per symbol respectively. The constellation is normally symmetrical, both the in-phase **I** and the quadrature **Q** component being modulated with the same number of bits. There are also exceptions, such as the 32-QAM modulation encountered in the DAB standard [19], where 3 bits modulate the **I** component and 2 bits the **Q** component.

The discrete amplitude modulation of the **I/Q** components is also referred to as amplitude shift keying or ASK. For example, the 64-QAM modulation consists of two independent 8-ASK modulations. In the 8-ASK modulation, every group of 3 input bits is assigned one of eight equally spaced discrete values. The mapping can be either binary or Gray encoded, as shown in **Figure 3.3**

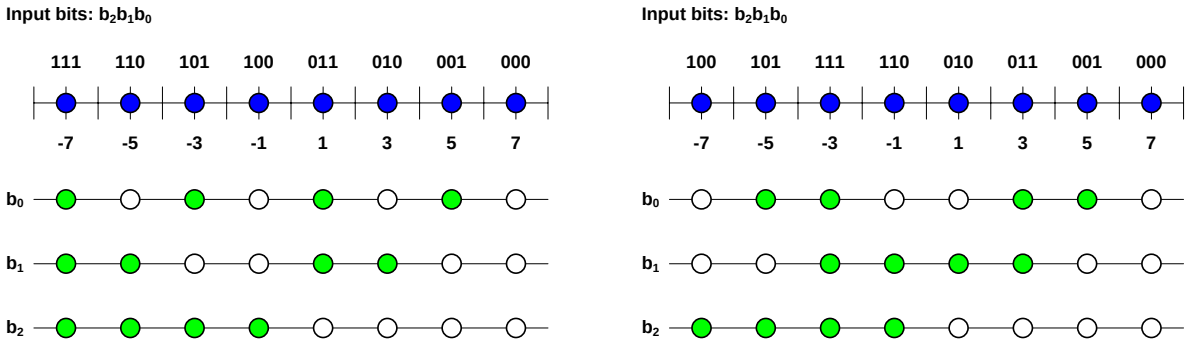

(a) Binary mapping (b) Gray mapping

Figure 3.3.: Mapping types for the 8-ASK modulation

The three input bits produce different partitions, depending on the specific mapping. An important property of a mapping is the bit distance, which is defined for each bit as the distance between the group of values for which the bit is 0 and the group for which the bit is 1. A larger bit group distance ensures a higher robustness against noise.

The Gray mapping has the advantage of a larger bit distance for the b_1 and b_0 LSB's, which makes it preferable in most digital broadcasting applications. On the other hand, binary encoding offers better performance when used in conjunction with iterative decoding [40], as in the DRM standard [21]. Iterative decoding, however, has the disadvantage of an increased latency and complexity, which make it practical only for relatively low data rates.

The actual complex QAM symbols S are formed by multiplying the mapping result $I + jQ$ by a normalization factor K_{mod}, as described by (**3.17**). The purpose of the normalization is to achieve the same average power for all modulation types. **Table 3.4** lists the normalization factors for three common modulation types: 4-QAM, 16-QAM, and 64-QAM. For practical implementations, most standards permit the use of approximate normalization factors, according to the specific bitwidth of the quantized signal.

$$S = (I + jQ) \times K_{mod} \tag{3.17}$$

In the following, the number of bits mapped on a subcarrier will be denoted by N_{bpsc}.

Modulation	K_{mod}
4-QAM	$1/\sqrt{2}$
16-QAM	$1/\sqrt{10}$
64-QAM	$1/\sqrt{42}$

Figure 3.4.: Normalization factors for QAM modulation

3.2.2. Interleaving

Interleaving is a process whereby the order of the symbols in a data stream is changed in order to provide resilience against burst errors on the channel. Unlike isolated errors, burst errors are much harder to correct with regular error correcting codes, either block and convolutional. In the receiver, the deinterleaving effectively spreads the burst of consecutive corrupted bits so that they can be more easily corrected by the FEC decoder.

In the specific case of OFDM with QAM modulation, the interleaving process must ensure that adjacent coded bits are mapped on non-adjacent subcarriers and alternatingly on the most and least significant bits of the QAM constellation. The first condition ensures that a group of

adjacent subcarriers affected by a deep fading does not result in an error burst, while the latter avoids long runs of low-reliability LSB's.

According to their principle of operation, interleavers can be divided into convolutional and block-based. Block interleavers essentially perform a permutation of the elements. Depending on how the permutation coefficients are generated, we distinguish matrix, random, and algebraic interleavers.

In matrix interleavers, the input symbols are written to a matrix row and read column by column. The block size is limited to values that can be expressed as $M \times N$. Random interleavers generate the permutation indices using an LFSR, whose length must accommodate the block size. If the block size is not a power of two, the addresses generated by the LFSR which exceed the block size will be ignored. In algebraic interleavers, the permutation table is generated using an algebraic equation.

In OFDM applications, where QAM data cells are mapped to OFDM symbols, block interleaving is the most straightforward solution. The cell interleaver is a mandatory component of any OFDM system, for both broadcasting and wireless networks. Some standards, such as DVB-T, may specify additional interleaving, depending on their particular FEC codes. Some others, such as DRM, group more OFDM symbols into an interleaving block, which offers slightly better performance for time-variant channels, at the cost of increased latency and memory requirements.

3.3. Broadcasting OFDM Receivers

3.3.1. Receiver Structure

An OFDM receiver is usually divided into an inner receiver and an outer receiver, as in **Figure 3.5**. The inner receiver performs the OFDM demodulation and channel estimation, providing the demodulated data $Z_{s,k}$ and the channel estimate samples $\tilde{H}_{s,k}$ to the outer receiver. The latter performs channel correction, QAM demapping and FEC decoding.

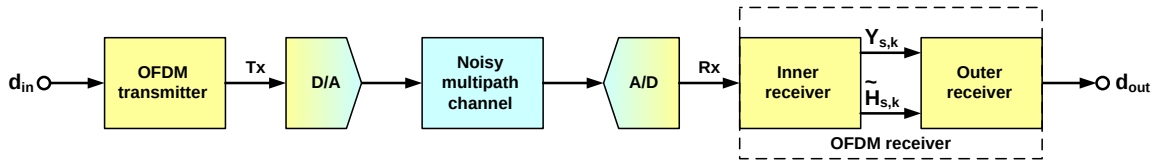

Figure 3.5.: Baseband transmission model

The inner receiver should minimize the synchronization errors and reduce the channel estimation errors. While the timing and frequency synchronization errors can be minimized through careful design, the inter-carrier interference (ICI) due to Doppler spread cannot be compensated and

will appear as additive noise on the demodulated signal. This effect is the main cause of performance degradation at high receiver speeds. A typical architecture of the inner receiver is shown in **Figure 3.6**. Note that the last stage is the channel estimation, the channel correction being included in the outer receiver. In some cases, an estimate of the noise variance is also provided to the outer receiver, which is useful for adapting the QAM demapping characteristic and for maximum-ratio combining in diversity receivers.

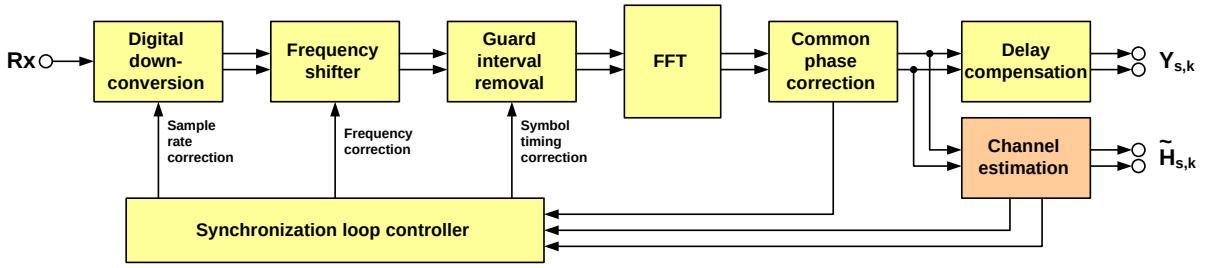

Figure 3.6.: Typical inner OFDM receiver for broadcasting

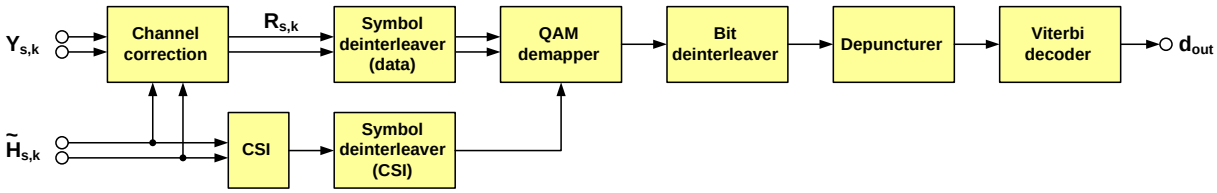

Figure 3.7.: Outer OFDM receiver for DVB-T

Channel estimation using scattered pilots is treated in more detail in **Chapter 5**. Special attention is given to the minimization of the interpolation error and to the noise reduction of the estimate, while still ensuring an acceptable computational complexity.

3.3.2. QAM Demapping

In the case of single-carrier systems, all data symbols are affected by the same noise power in average. Therefore, the reliability of a received signal is proportional to the distance from the constellation decision boundary. This value is then used as a soft-decision value for FEC decoding (computing the branch metrics in the case of Viterbi decoding).

It has been showed that near-optimal decoding requires that the soft-decision values be equal with the log-likelihood ratio (LLR) associated with each bit [77]. Denoting the received value by r, the LLR of demapped bit b_m is defined as:

$$LLR(b_m) \triangleq \log \frac{P\{b_m = 1|r\}}{P\{b_m = 0|r\}} \tag{3.18}$$

where $P\{b_m = 1|r\}$ is the a-priori probability that $b_m = 1$ was transmitted when receiving r, and m is the index of the bit in a multi-bit symbol. For instance, when demapping 4-ASK, $m = \{0, 1\}$, while for 8-ASK $m = \{0, 1, 2\}$.

Assuming the transmitted constellation points α have equal probability and applying the Bayes rule that links the a-priori to the a-posteriori probability, the following expression of the LLR results for bit b_m:

$$LLR(b_m) = \log \frac{\sum_{\alpha \in \mathcal{S}_m^1} P\{r|a=\alpha\}}{\sum_{\alpha \in \mathcal{S}_m^0} P\{r|a=\alpha\}} \tag{3.19}$$

where a are the original transmitted symbols belonging to the alphabet α. In the above equation, we denoted by $\mathcal{S}_m^1$ and $\mathcal{S}_m^0$ the discrete set of constellation points α for which b_m is 1 and 0 respectively. **Figure 3.8** shows the partitions for 8-ASK modulation (I/Q for 64-QAM) when using binary and Gray encoding.

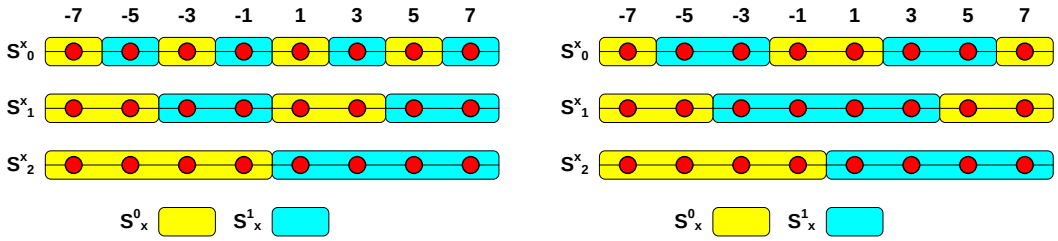

(a) Binary encoding (b) Gray encoding

Figure 3.8.: $\mathcal{S}_m^0$ and $\mathcal{S}_m^1$ partitions for 8-ASK mapping (64-QAM)

For high SNR ratios, the received symbols a are grouped around constellation points α and the following log-sum approximation can be made: $\log \sum_i x_i \approx \max_i \log x_i$. The LLR can now be expressed as:

$$LLR(b_m) \approx \log \frac{\max_{\alpha \in \mathcal{S}_m^1} P\{r|a=\alpha\}}{\max_{\alpha \in \mathcal{S}_m^0} P\{r|a=\alpha\}} \tag{3.20}$$

If the noise affecting the received symbols r is Gaussian with variance σ^2, the a-posteriori probability $P\{r|a=\alpha\}$ can be expressed as:

$$P\{r|a=\alpha\} = \frac{1}{\sqrt{2\pi}\sigma} \exp\left(-\frac{|r-\alpha|^2}{2\sigma^2}\right) \tag{3.21}$$

Using (**3.21**) in (**3.20**), the soft metrics can be expressed as:

$$LLR(b_m) = \frac{1}{4}\left(\min_{\alpha \in \mathcal{S}_m^0} |r-\alpha|^2 - \min_{\alpha \in \mathcal{S}_m^1} |r-\alpha|^2\right) \triangleq D_m \tag{3.22}$$

The soft metrics are obtained by computing the difference between the quadratic distances from the received symbol r to the closest constellation points α belonging to the two sets $\mathcal{S}_m^0$ and $\mathcal{S}_m^1$ respectively. **Figure 3.9** shows the three soft metrics in the case of 8-ASK (64-QAM) demapping, for both binary and Gray encoding.

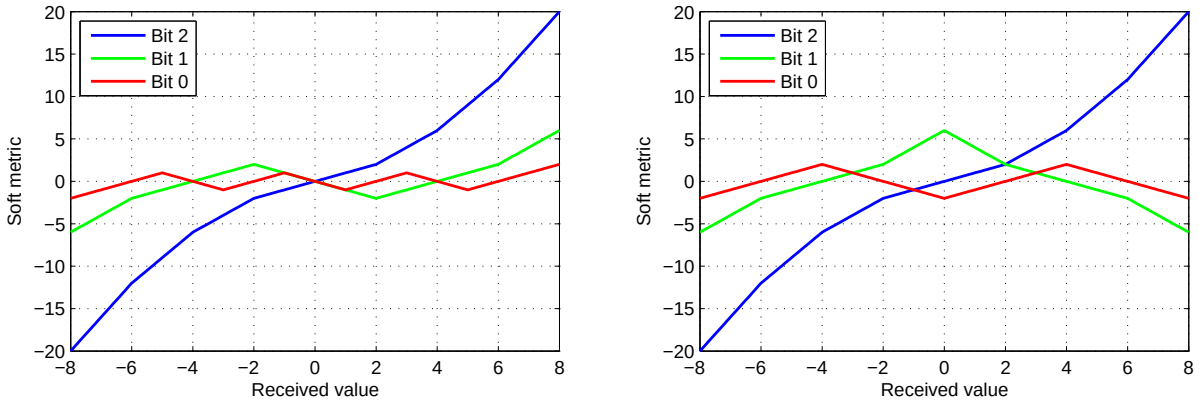

(a) Binary encoding (b) Gray encoding

Figure 3.9.: Accurate soft metrics generation for 8-ASK (64-QAM)

For Gray constellation encoding, which is the regular case used in non-multi-level mapping, such as in DVB-T, the expression for D_m in the case of 8-ASK can be expressed according to [89, 77] as:

$$D_2 = \begin{cases} r & |r| \leqslant 2 \\ 2(r - 1 \cdot \text{sign}(r)) & 2 < |r| \leqslant 4 \\ 3(r - 2 \cdot \text{sign}(r)) & 4 < |r| \leqslant 6 \\ 4(r - 3 \cdot \text{sign}(r)) & |r| > 6 \end{cases} \tag{3.23}$$

$$D_1 = \begin{cases} 2(-|r| + 3) & |r| \leqslant 2 \\ 4 - |r| & 2 < |r| \leqslant 6 \\ 2(-|r| + 5) & |r| > 6 \end{cases} \tag{3.24}$$

$$D_0 = \begin{cases} |r| - 2 & |r| \leqslant 4 \\ -|r| + 6 & |r| > 4 \end{cases} \tag{3.25}$$

The above equations lead to a relatively complex implementation. Fortunately, the complexity can be reduced by using a set of approximative equations for D_m, as in [89, 70]:

$$D_2 = r \tag{3.26}$$

$$D_1 = -|r| + 4 \tag{3.27}$$

$$D_0 = -||r| - 4| + 2 \tag{3.28}$$

The new soft metrics are shown in **Figure 3.10** as a function of the input value in range $[-8; 8]$. The approximated D_m represent the distance of the received symbol r from the nearest partition boundary, the sign depending on the partition in which r is located. Equation (**3.26**)

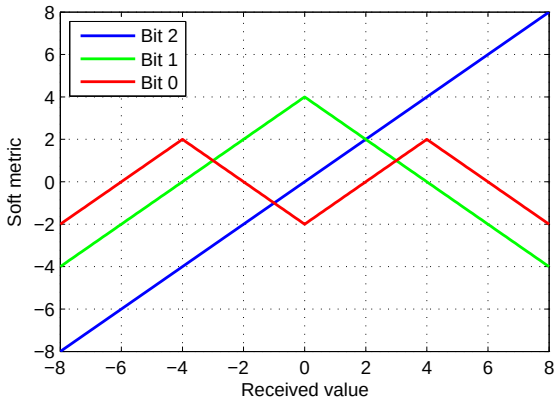

Figure 3.10.: Soft metrics generation for 8-ASK using the approximate linear method

can also be expressed recursively as:

$$D_m = \begin{cases} r & m = M-1 \\ 2^{m+1} - |D_{m+1}| & 0 \leqslant m < M-1 \end{cases} \tag{3.29}$$

where M is the number of bits per ASK symbol. The equation holds for any Gray ASK mappings of all sizes. The recursive definition of D_m greatly simplifies the hardware implementation by allowing the generation of all soft metrics sequentially using a single adder. An additional advantage of the simplified metrics is that the output range is narrower (cf. **Figure 3.9b** and **Figure 3.10**), which reduces the number of bits required for the discrete metrics.

Simulations have shown that the simplified metrics introduce no BER degradation compared to the "ideal" metrics computed according to (**3.22**). **Figure 3.11** shows the BER as a function of SNR, in the case of 64-QAM mapping with Gray encoding for AWGN channels and a coding rate of 1/2, using soft and hard metrics. Soft QAM demapping greatly improves performance, with gains of at least 3 dB for the same BER value.

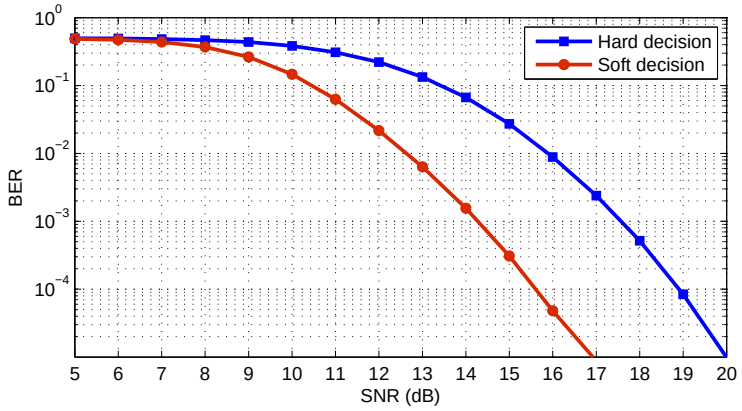

Figure 3.11.: BER for 64-QAM and 1/2 code rate with AWGN channel

Figure 3.12 shows the BER-vs-SNR curves for the three types of QAM constellations in an AWGN channel, using a convolutional code rate of 1/2. QAM demapping is performed using soft metrics.

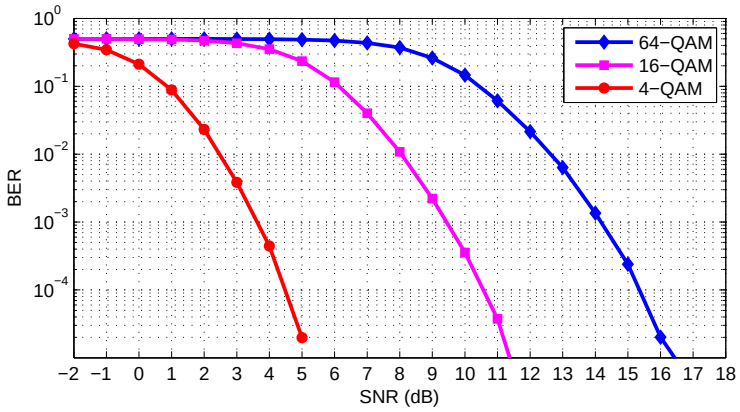

Figure 3.12.: BER for 1/2 code rate and various QAM constellations with AWGN channel

So far, the discussion was confined to the case of AWGN channels. In the case of OFDM systems operating in multi-path channels, all data symbols are not affected by the same noise power. As the channel is frequency-selective, the attenuation experienced by the subcarriers will vary, so that those carriers that experience deep fading will have a degraded signal-to-noise ratio (SNR) compared to those on a channel transfer function (CTF) peak. Thus, data on a CTF high will be more reliable that data on a CTF low. The additional reliability information is referred to as channel state information (CSI) and must be considered when generating the soft metrics in the QAM demapping process.

In order to determine the expression of the CSI, we express the equalized data as $y_k = H_k \cdot r_k$, where k is the subcarrier index and H_k is the channel transfer function (CTF) at subcarrier k. In a frequency-selective channel (**3.30**) becomes:

$$P\{r_k|a_k = \alpha\} = \frac{1}{\sqrt{2\pi}\sigma} \exp\left(-\frac{|r_k - H_k\alpha_k|^2}{2\sigma^2}\right) \tag{3.30}$$

The soft metrics in (**3.22**) are now expressed as:

$$D_m = \frac{|H_k|^2}{4}\left(\min_{\alpha\in\mathcal{S}_m^0} |y_k - \alpha|^2 - \min_{\alpha\in\mathcal{S}_m^1} |y_k - \alpha|^2\right) \tag{3.31}$$

The soft metrics need to be multiplied with the CSI, which is the square of the absolute value of the CTF, according to the above equation. Low absolute values of the CTF indicate that the error of the equalized data is high. Simulations have shown that the decoding performance is not degraded if the CSI is only the absolute value of the CTF, not its square. In a practical realization, the absolute value of the CTF is already needed for equalization, so that no extra hardware is necessary, apart from an additional symbol deinterleaver.

Weighting the soft metrics with the CSI greatly improves the decoding performance, as shown in **Figure 3.13** for a DVB-T system in 2K mode with a code rate of 1/2 and interleaving operating in a Rayleigh multi-path channel with three taps of equal amplitude. The actual channel profile only affects the results slightly, and only due to second-order effects.

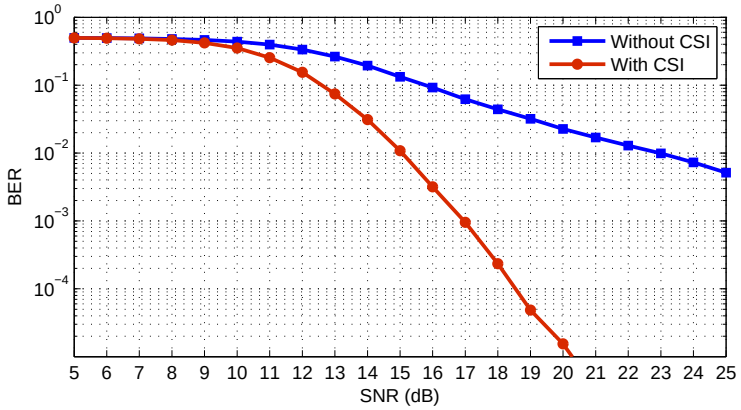

Figure 3.13.: BER for 64-QAM and 1/2 code rate and interleaving in Rayleigh channel

Another solution for computing the CSI was proposed in [70], which relies on using the MSE of the pilots after channel equalization. For good and moderate values of SNR, the MSE of the equalized pilots can be approximated as their imaginary part. The CSI is obtained by interpolating between the inverse of the MSE's at the pilot positions. This solution requires an additional division and interpolation stage, while providing no performance gain. We therefore chose to derive the CSI information as the absolute value of the CTF.

3.4. Broadcasting Standards that Use OFDM

3.4.1. DVB-T

OFDM Modulation

The OFDM signal is organized in frames, each frame having 68 OFDM symbols. Four frames constitute one super-frame. The number of active carriers per symbol is K = 6817 in the 8K mode and K = 1705 in the 2K mode. Four guard interval lengths are specified for each mode, as shown in **Table 3.1**, which covers a wide range of requirements.

The baseband sample frequency f_s is: 64/7 MHz for 8 MHz channels, 8 MHz for 7 MHz channels, 48/7 for 6 MHz channels, and 40/7 MHz for 5 MHz channels. All timing parameters are expressed in sampling periods $T = 1/f_s$.

Besides data cells, the OFDM frame contains pilot cells (scattered and continual) and TPS

Parameter	8K mode	2K mode
Symbol size N_U	8192 (2^{13})	2048 (2^{11})
Guard interval N_G/N_U	1/4, 1/8, 1/16, 1/32	
Active subcarriers $\{K_{min}; K_{max}\}$	$\{-3408; +3408\}$	$\{-852; +852\}$
Scattered pilots spacing $\{D_K; D_S\}$	$\{3; 4\}$	

Table 3.1.: OFDM parameters of DVB-T

carriers for transmission parameter signaling. The pilots are transmitted at a boosted power level $E\{c \times c^*\}$ of 16/9, unlike other cells that have an average power level of 1.

The values of the pilot cells are derived from a PRBS sequence w_k, corresponding to their carrier index k, which is generated using an LFSR with generator polynomial $X^{11} + X^2 + 1$. The generator is initialized on the first active carrier and is incremented every active carrier. The modulation of the pilots is given by:

$$Re\{c\} = \begin{cases} +4/3 & \text{when } w_k = 0 \\ -4/3 & \text{when } w_k = 1 \end{cases} \tag{3.32}$$

$$Im\{c\} = 0 \tag{3.33}$$

The number of continual pilots is 177 in 2K mode and 177 in 8K mode. Their spacing is not regular, but is always a multiple of $D_K = 3$. Each continual pilot coincides with a scattered pilot every $D_S = 4$ OFDM symbols.

The TPS carriers are used for conveying the transmission parameters, such as channel coding and modulation. TPS are transmitted in parallel using 17 dedicated carriers in 2K mode and 68 carriers in 8K mode. Every TPS carrier in a symbol conveys the same data bit, which ensures an extremely robust decoding of the TPS information.

A TPS block consists of 67 bits, differentially encoded over the 68 consecutive symbols of an OFDM frame using 2-PSK modulation. The initial phase is generated with the same PRBS sequence used for modulating the pilots. Of the 67 bits, the first 16 bits are used for synchronization, 37 bits carry the payload, and the last 14 bits are BCH parity.

Channel Coding

According to the MPEG-2 standard, the transport data stream is organized in fixed-length (188 bytes) packets, following the transport multiplexor, the start of a packet being marked by the synchronization byte 47_{HEX}. Stream bytes are then fed to the DVB-T modulator with the MSB first.

In order to destroy any periodic patterns and ensure adequate binary transitions, the input data stream is randomized (scrambled) using a pseudo random binary sequence (PRBS) implemented using a linear feedback shift register (LFSR) with the following generator polynomial: $1+X^{14}+X^{15}$. The LFSR is initialized every eight transport packets on the sync word. The sync words are not unscrambled.

The scrambled bit stream is then FEC encoded and interleaved. FEC encoding is performed in two stages, using and outer Reed-Solomon code and an inner convolutional code. Interleaving is performed after each coding stage.

The outer coding and interleaving is performed on 188-byte packets. The code used is a shortened Reed-Solomon RS(204,188,t=8) code derived from the original systematic RS(255,239,t=8) code by adding 51 null bytes and discarding them after encoding. Thus, the RS encoder appends 16 parity bits to a 188-byte packet. Such a code can correct up to 8 random bytes in a 204-byte received symbol. The sync words are also considered in the RS encoding.

Following the RS block encoding, a convolutional byte-wise interleaving is performed, using a Forney approach. The interleaver consists of I = 12 branches which are cyclically connected to the input stream by a switch. Each branch j is a shift register with a delay of j×M, where M = 17 = N/I, N = 204. The output switch is synchronized with the input switch, with the sync byte of the 204-byte packet being routed to branch 0.

The inner coding is based on a mother convolutional code with a constraint length of 6 and 2 output branches, using the following generator polynomials: $G_1 = 171_{OCT}$, $G_2 = 133_{OCT}$. In addition to the mother code of rate 1/2, the following punctured rates are defined: 2/3, 3/4, 5/6, 7/8, the corresponding puncturing patterns being defined in **Figure 3.14**. Using puncturing, coding efficiency can be traded-off for robustness against errors.

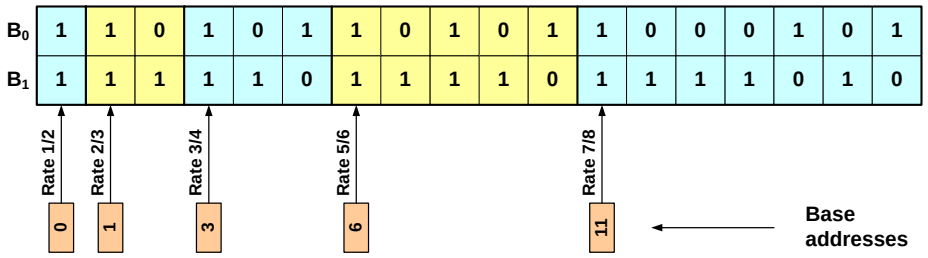

Figure 3.14.: Puncturing patterns in DVB-T

Following the inner encoding, the inner interleaving is performed, which consists of bit-wise interleaving followed by symbol interleaving. Both interleaving processes are block based. In the following, only the non-hierarchical mode is described.

For bit-wise interleaving, the input is demultiplexed into v sub-streams, where v is the number of bits per constellation symbol, e.g. v = 6 for 64-QAM. The demultiplexing is shown in **Figure 3.15**, together with the bit-wise and symbol interleaving. Each bitstream undergoes a separate interleaving, therefore up to 6 interleavers are required. The block size is 126 bits

Stream	Interleaving function
I0	$H_0(w) = w$
I1	$H_1(w) = (w + 63) \mod 126$
I2	$H_2(w) = (w + 105) \mod 126$
I3	$H_3(w) = (w + 42) \mod 126$
I4	$H_4(w) = (w + 21) \mod 126$
I5	$H_5(w) = (w + 84) \mod 126$

Table 3.2.: Permutation functions for bit-interleaving in DVB-T

for all interleavers. Thus, the interleaving process is repeated exactly 12 times in the 2K mode and 48 times in the 8K mode. The permutation function is defined by the equation:

$$a_{e,w} = b_{e,H_e(w)} \qquad w = 0, 1, 2, \ldots, 125 \tag{3.34}$$

where e is the interleaver index and $H_e(w)$ is a permutation function which is different for each interleaver, as defined in **Table 3.2**.

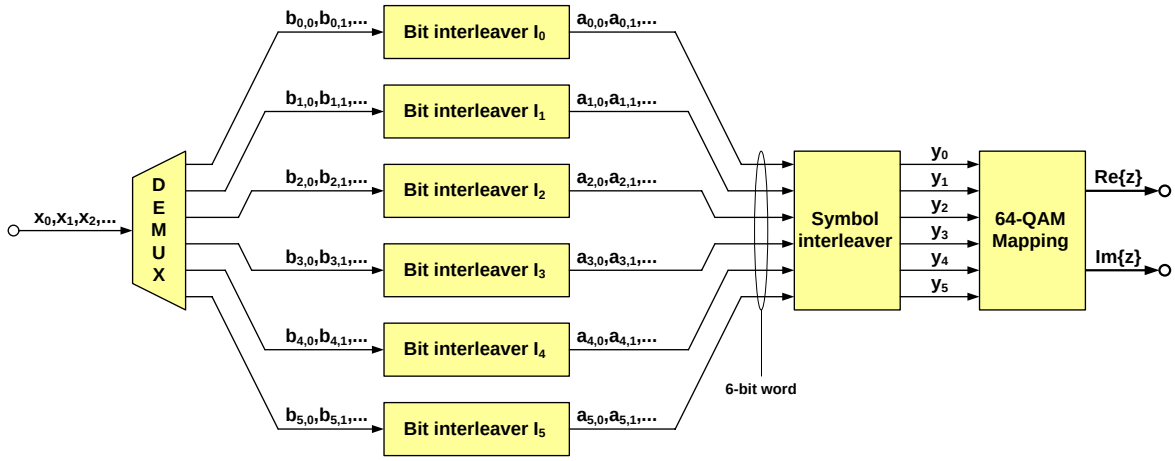

Figure 3.15.: Bit and symbol interleaving in DVB-T

The symbol interleaver maps v-bit words onto the active subcarriers of an OFDM symbol, the block size N_{max} being 1512 in the 2K mode and 6048 in the 8K mode. The interleaving is described by the following equations:

$$y_{H(q)} = y'_q \qquad \text{for even symbols} \tag{3.35}$$

$$y_q = y'_{H(q)} \qquad \text{for odd symbols} \tag{3.36}$$

where $q = 0, 1, \ldots, N_{max} - 1$. The permutation $H(q)$ is generated using an LFSR random generator and an additional wired permutation. **Figure 3.16** shows the permutation generator for

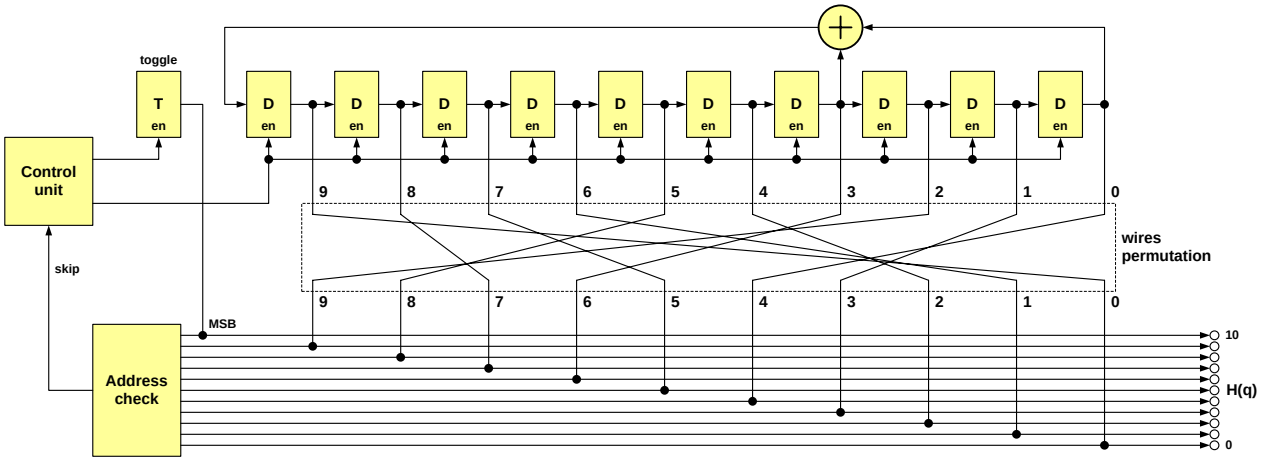

Figure 3.16.: $H(q)$ address generator for symbol interleaving in DVB-T

the 2K mode. The generator polynomials and the exact expressions for the wired permutations are given in [20].

Following the symbol interleaver, the v-bit words are mapped on the constellation. Three QAM constellations are defined by the DVB-T standard: 4-QAM (QPSK), 16-QAM, and 64-QAM. The even bits generate the in-phase component $Re\{z\}$, while the odd bits generate the quadrature component $Im\{z\}$, using ASK Gray mapping as shown in **Figure 3.3b**. The mapping of the word bits $y_0, y_1, y_2, y_3, y_4, y_5$ for 64-QAM is shown in **Figure 3.17**. A similar mapping principle is used for 16-QAM.

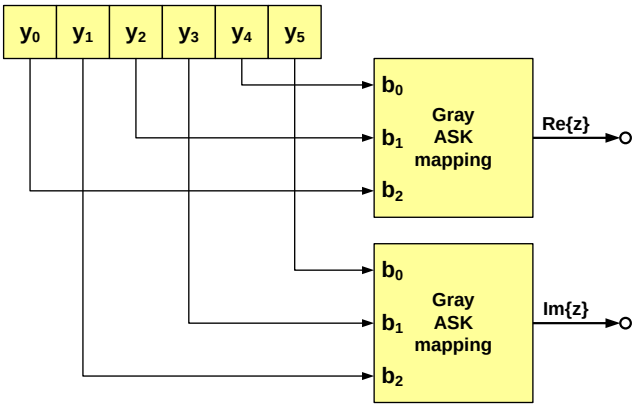

Figure 3.17.: 64-QAM mapping in DVB-T

3.4.2. DRM

Digital Radio Mondiale (DRM) is an OFDM digital audio broadcasting system for the traditional AM bands below 30 MHz. The standard is non-proprietary and has been developed

by an international consortium [21]. Unlike FM bands, AM bands allow the coverage of large or remote areas, which is essential for international broadcasting. At the same time, DRM offers much better sound quality compared to AM transmissions, with the benefit of additional information and data services.

DRM is fully compatible with the current ITU spectrum regulations for LW, MW and SW, which specify a channel bandwidth of 9 or 10 KHz. For a good audio quality, state-of-the-art algorithms can compress an audio stream to a rate of 20 to 24 kbit/s, which requires a spectral efficiency of at least 2 bit/s/Hz. Considering the pilot symbols, the channel coding and the signaling overhead, a 64-QAM modulation scheme becomes mandatory. For severe multi-path and Doppler effects, achieving the required SNR required by such a large constellation becomes a tough design task.

Another design challenge is the complexity of the standard. Although the available datarates are relatively low, the receiver complexity is even greater than for DVB-T. Among the factors that contribute to this complexity are the support for different robustness modes, bandwidths, and data rates, in conjunction with powerful multi-level channel coding. Moreover, the mapping scheme, the code rates, and the stream partitioning can be changed dynamically during operation. These considerations also make the DRM receiver an ideal application for reconfigurable design.

OFDM Modulation

DRM is designed to operate at frequencies below 30 MHz, with a nominal bandwidth of 9 kHz or 10 kHz. The standard also makes provision for transmissions using half (4.5 kHz or 5 kHz) or twice (18 kHz or 20 kHz) these bandwidths. In order to allow for different propagation conditions, four robustness modes (A, B, C, an D) are specified. Choosing a certain mode is a trade-off between spectral efficiency and ruggedness to delay and Doppler spread.

The four robustness modes differ in their OFDM symbol and cyclic prefix length, as shown in **Table 3.3**. In this table, T_g, T_s and T_u are the durations of the guard interval, the OFDM symbol, and its useful part respectively. These parameters are expressed in terms of elementary period $T = 83\frac{1}{3}$. The OFDM symbols are grouped in frames of constant duration $T_f = 400$ ms. It follows that the number of symbols per frame depends on the mode, as show in **Table 3.3**. Three transmission frames are grouped to form a super frame.

By combining the four robustness modes with the six spectrum occupancies, various data rates can be achieved. However, not all 24 combinations are allowed, mode C and D (for severe multipath effects) being available only for 10 kHz and 20 kHz bandwidths. One can also observe that the symbol sizes are not always powers-of-2, which complicates the implementation since the FFT algorithm cannot be applied. The DRM frame consists of data, control, and pilot cells.

There are three types of pilot cells: frequency, time, and gain references. *Frequency references*

Robustness	Mode A	Mode B	Mode C	Mode D
T_u	$288 \times T$	$256 \times T$	$176 \times T$	$112 \times T$
T_g	$32 \times T$	$64 \times T$	$64 \times T$	$68 \times T$
$T_s = T_u + T_g$	$26\frac{2}{3}$ ms	$26\frac{2}{3}$ ms	20 ms	$16\frac{2}{3}$ ms
Carrier spacing $1/T_u$	$41\frac{2}{3}$ Hz	$46\frac{7}{8}$ Hz	$68\frac{2}{11}$ Hz	$107\frac{1}{7}$ Hz
T_g/T_u	1/9	1/4	4/11	11/14
Symbols per frame	15	15	20	24

Table 3.3.: OFDM parameters

are transmitted on 750 Hz, 2250 Hz and 3000 Hz regardless of the robustness mode, with cell phases chosen to ensure continuity at symbol boundaries. They can be used for frequency offset estimation in frequency synchronization algorithms. **Figure 3.18** shows the real part of the three frequency references in time domain for Mode A and Mode B.

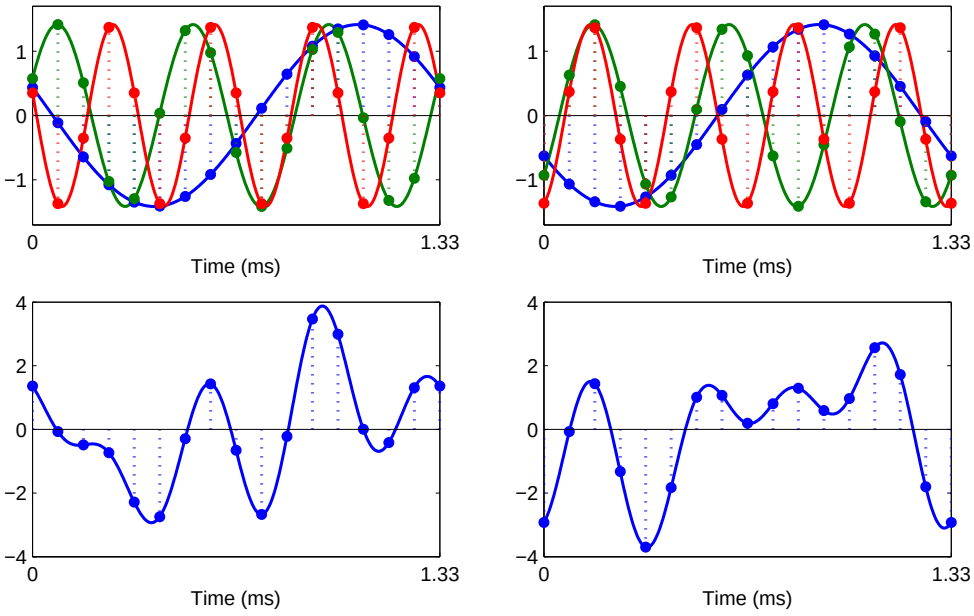

(a) Mode A (b) Mode B

Figure 3.18.: DRM frequency references in time domain

Time references are located in the first symbol of each frame, being used for the identification of frame boundaries. *Gain references* are scattered throughout the time-frequency grid and are used for channel response estimation. Depending on the robustness mode, between 1/20 to 1/3 of the cells are used as scattered pilots.

Besides the reference cells, DRM frames contain three types of information cells, corresponding

to FAC (fast access channel), SDC (service description channel), and MSC (multiplex service channel) which contains the actual transport streams. **Figure 3.19** shows their allocation within a super frame.

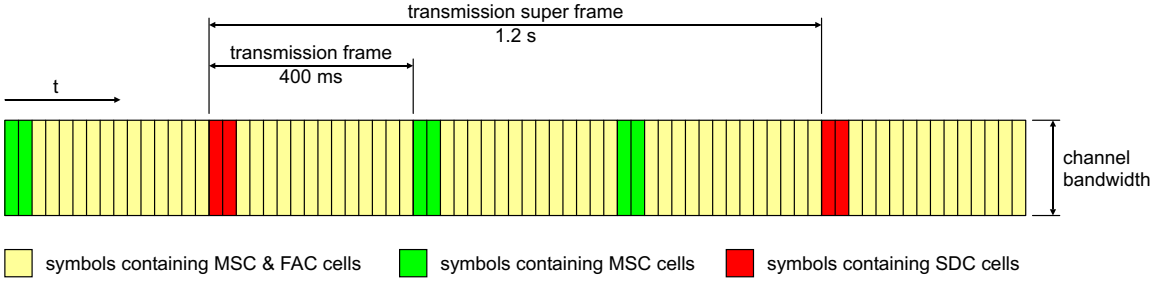

Figure 3.19.: Cell mapping on the DRM super frame

A transmission super frame contains one SDC block of N_{SDC} cells, three FAC blocks of N_{FAC} cells each and three MSC blocks of N_{MUX} cells each (multiplex frame). The FAC contains information about the channel parameters, such as the modulation types for SDC and MSC, and about the services in the multiplex. The SDC provides various signaling functions and information on how to decode the MSC (code rates and block sizes).

Channel Coding

Before being mapped on the DRM super frame, the MSC data is block interleaved, with a block size of N_{NUM} or $3 \times N_{NUM}$, where N_{NUM} denotes the number of MSC data cells per frame. The interleaving depth is chosen according to the predicted propagation conditions. The largest block size is 18354 cells, which is achieved for Mode A with 20 kHz bandwidth and long interleaving.

The next step in decoding is the QAM demapping and the MLC decoding. Because different bits in a QAM symbol are differently affected by noise, DRM employs a multilevel coding (MLC) scheme, which consists in the joint optimization of the QAM modulation and coding rate. For example, if 64-QAM is used, the input stream is divided into three streams which are encoded with different rates. The main constraint is that after convolutional encoding and puncturing, the three streams must have the same length. The DRM standard specifies different constellations, mapping types and code rates, which results in a wide range of data rates and complicates the design.

For the FAC, 4-QAM mapping is used, with a code rate of 0.6. The SDC uses 4-QAM or 16-QAM mapping, with a code rate of 0.5 in both cases. The MSC uses 16-QAM or 64-QAM, with three mapping modes for the latter. For each case, different protection levels (code rates) are specified, which results in a wide range of data rates. Various code rates are obtained by using different puncturing patterns. The DRM standard defines 13 puncturing patterns for the regular stream, plus 24 additional ones for trellis termination at the end of the block to achieve

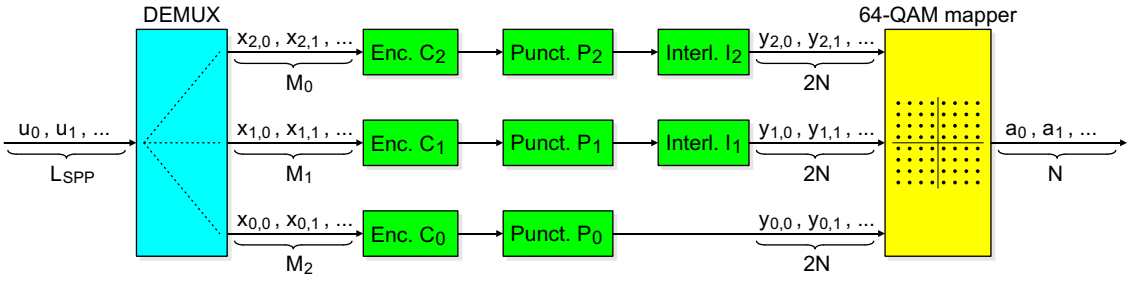

Figure 3.20.: Multilevel coding for 64-QAM in DRM

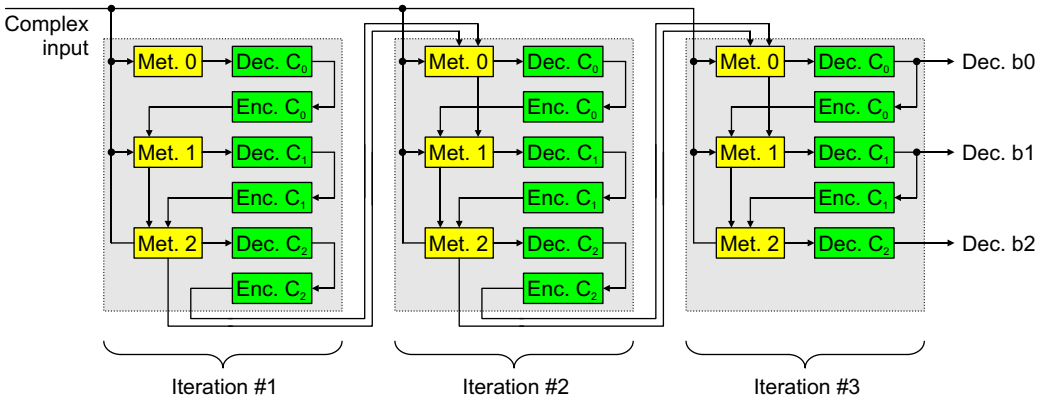

Figure 3.21.: Iterative multilevel decoding for 64-QAM in DRM

an exact data rate. The latter are presented in **Figure 3.23**.

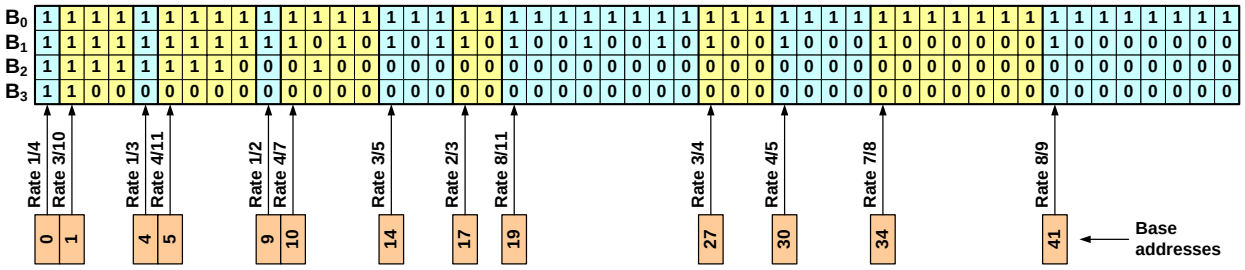

Figure 3.22.: Main puncturing patterns in DRM

Another special feature of the DRM standard is that the source can be encoded into two parts with unequal protection levels. As the audible effects of errors are not the same for all parts of the stream, more sensitive information is transmitted with a higher protection than the less sensitive information. This allows for "graceful degradation" of the audio quality when reception conditions worsen.

In order to achieve near FM quality at such low bandwidths, sophisticated audio encoding algorithms have been used, namely a subset of the MPEG-4 AAC toolbox. Besides AAC, DRM also supports CELP and HVXC speech coding to allow for reasonable quality at very low

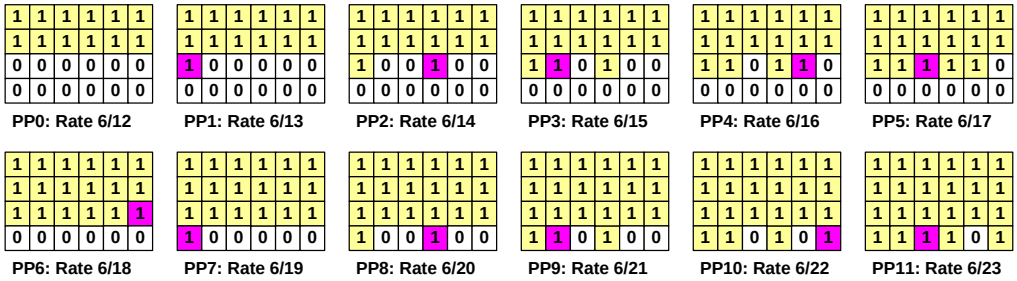

Figure 3.23.: Puncturing patterns of the tail-bits in DRM

data rates. To further improve audio quality, spectral band replication (SBR) can be used in conjunction with all three codings. When using AAC + SBR, parametric stereo (PS) coding can add stereo quality with a minimal increase in bit-rate. Because of the complexity of such algorithms, a software implementation is the only realistic approach.

Also say something about the interleaving.

3.4.3. IEEE 802.16a

The IEEE 802.16 wireless MAN standard [39] specifies a PHY for multiple access based on OFDM, which is designed for NLOS (non-line-of-sight) operation in the frequency bands below 11 GHz. The OFDMA PHY is specified by the IEEE 802.11a standard.

Although it is a wireless networking standard, the downlink (DL) path from the base station (BS) to the subscriber station (SS) has the same modulation principles like a broadcasting channel. Instead of a packet-based burst transmission, the BS sends a continuous data stream, with scattered pilots, much like a broadcasting transmitter. The SS will demodulate this data stream and extract exactly the data slices allocated to it.

OFDM Modulation

The active carriers are grouped into subsets, referred to as subchannels. In DL, a subchannel may carry data for different SS; in UL, a SS may be assigned one or more subchannels, with several SS being able to transmit simultaneously [39]. The grouping into subchannels is shown in **Figure 3.25**. The baseband DC carrier is suppressed.

Duplex operation is implemented using either frequency-division (FDD) or time-division (TDD). FDD systems may be also half-duplex. In licensed bands, the duplexing method can be either FDD or TDD. In license-exempt band, only TDD is allowed. **Figure 3.25** shows an example of DL and UL allocation in the case of TDD.

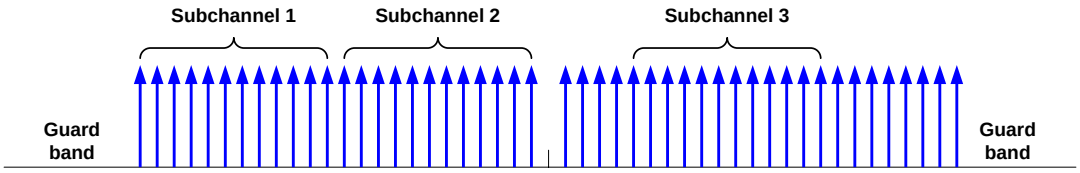

Figure 3.24.: OFDMA subchannel carrier allocation for IEEE 802.16a

The symbol structure and thus the data mapping is different for DL and UL, as well as for PUSC and FUSC. OFDM cells are organized into data slots, with a size of one subchannel by one to three OFDM symbols. Data slots in turn are grouped into data regions (shown in **Figure 3.25** as bursts), which are the basic units of MAC data allocation. As it can be seen, the allocation is different in DL and UL

Subchannel allocation in DL can be performed with partial usage of the subchannel (PUSC), where only some of the subchannels are allocated to the transmitter, or with full usage of the subchannels (FUSC), where all subcarriers are allocated. FUSC is only used in DL, whereas PUSC can be used in both DL and UL. Subcarrier allocation differs greatly between PUSC and FUSC modes, as indicated below.

For FUSC, the pilot cells are allocated first. The remaining cells are used for data and divided into subchannels. For PUSC, the used subcarriers are first partitioned into subchannels. Pilot cells are then allocated within subchannels so that each subchannel contains its own set of pilots. It is now obvious that only the FUSC mode is similar to a broadcasting OFDM transmission as far as the channel estimation is concerned.

The OFDMA parameters for the FUSC in down-link are shown in **Table 3.4**. The IEEE 802.11a standard defines a mandatory and an optional carrier allocation, which only differ in their pilot distribution.

In the mandatory allocation, there are both scattered and continual pilots, each divided into two equal interleaved subsets. Unlike DVB-T and DRM, the continual and the scattered pilots do not overlap. In transmission diversity operation with two senders, each sender transmits only one set of pilots. The optional allocation only specifies scattered pilots, which have the D_k and D_s spacings different from the mandatory allocation. For both cases, the resulting number of data subcarriers is 1536, which are grouped into 32 subchannels of 48 carriers each. The mapping of logical to physical subchannels is not sequential but through a random-like permutation.

The sampling frequency f_s depends on the nominal channel bandwidth BW alone, according to the following formula:

$$f_s = \left\lfloor \frac{8/7 \cdot BW}{8000} \right\rfloor \times 8000 \tag{3.37}$$

where the $\lfloor \cdot \rfloor$ operator denotes the next smaller integer.

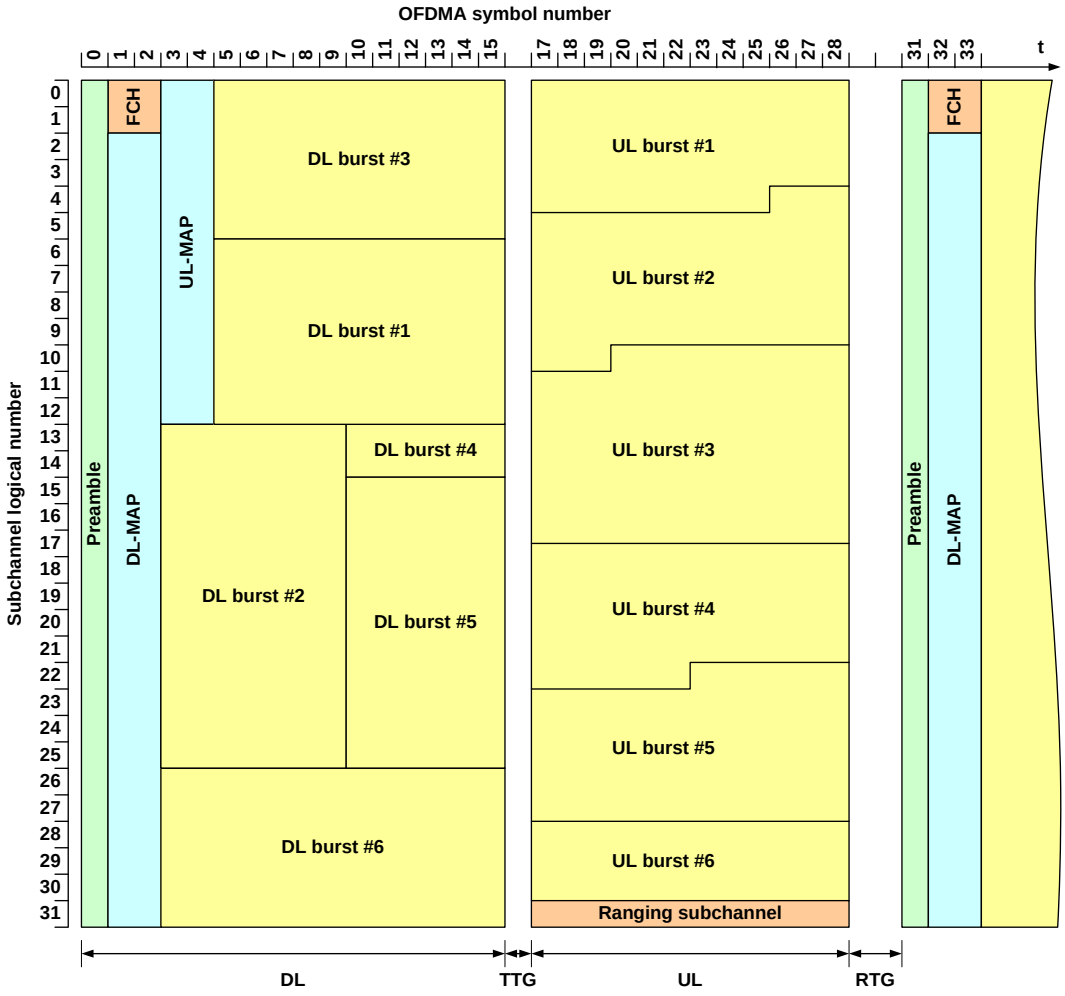

Figure 3.25.: Time-division duplexing and cell allocation for IEEE 802.16a

Parameter	mandatory mode	optional mode
Symbol size N_U	2048	
Guard interval ratio $G = N_G/N_U$	1/4, 1/8, 1/16, 1/32	
Number of active subcarriers	1702	1728
Active subcarriers $\{K_{min}; K_{max}\}$	$\{-851; +851\}$	$\{-864; +864\}$
Scattered pilots spacing $\{D_K; D_S\}$	$\{6; 2\}$	$\{3; 3\}$
Number of scattered pilots	142 (2×71)	192
Number of continual pilots	24 (2×12)	—
Number of data subcarriers	1536 (48×32)	
Number of data subcarriers per subchannel	48	
Number of subchannels	32	

Table 3.4.: OFDMA parameters for IEEE 802.16a